

## Method of Measuring High-LET Particles Dose

Maya Dymova,<sup>a,1</sup> Maria Dmitrieva,<sup>a</sup> Elena Kuligina,<sup>a</sup> Vladimir Richter,<sup>a</sup> Sergey Savinov,<sup>b</sup> Ivan Shchudlo,<sup>b</sup> Tatiana Sycheva,<sup>b</sup> Iuliia Taskaeva<sup>c,d</sup> and Sergey Taskaev<sup>b,d</sup>

<sup>a</sup> Institute of Chemical Biology and Fundamental Medicine, <sup>b</sup> Budker Institute of Nuclear Physics and <sup>d</sup> Research Institute of Clinical and Experimental Lymphology – Branch of the Institute of Cytology and Genetics, Siberian Branch of the Russian Academy of Sciences, Novosibirsk, Russia; and <sup>c</sup> Novosibirsk State University, Novosibirsk, Russia

---

Dymova, Maya, Dmitrieva, Maria, Kuligina, Elena, Richter, Vladimir, Savinov, Sergey, Shchudlo, Ivan, Sycheva, Tatiana, Taskaeva, Iuliia and Taskaev Sergey, Method of Measuring High-LET Particles Dose. *Radiat. Res.* **196**, 192–196 (2021).

In boron neutron capture therapy, the total absorbed dose is the sum of four dose components with different relative biological effectiveness (RBE): boron dose, “nitrogen” dose, fast neutron dose and  $\gamma$ -ray dose. We present a new approach for measuring the first three doses. In this work, we provide the details of this method of dose measurement and results when this proposed method is employed. © 2021 by Radiation Research Society

---

### INTRODUCTION

For any type of ionizing radiation, the primary processes that occur in the medium are ionization and excitation (1). Therefore, the biological effects observed under the influence of charged particles, neutrons and gamma quanta are not due to their physical nature, nor even more so to their source, but to the amount of absorbed energy and its spatial distribution, characterized by the linear energy transfer (LET). The higher the LET, the greater the degree of biological damage. This degree determines the relative biological effectiveness (RBE) of various types of radiation. In boron neutron capture therapy, the total absorbed dose is the sum of four dose components with different RBE: boron dose; high-LET dose from the  $^{14}\text{N}(\text{n},\text{p})^{14}\text{C}$  reaction (“nitrogen” dose); fast neutron dose; and  $\gamma$ -ray dose. As has been previously stated, “The first two dose components cannot be measured in principle” (2). The methods for measuring the fast neutron dose for BNCT are also absent, as the energy of neutrons, as a rule, is obviously lower than 1 MeV and, for example, fission ionization chambers are not applicable. However, quite a few proven approaches

exist for only measuring  $\gamma$ -ray dose. We present a new approach for measuring the equivalent dose components due to neutrons: nitrogen dose, and fast neutron dose.

Before describing the proposed approach for measuring, we detail the processes leading to these four doses:

Boron dose:  $^{10}\text{B}(\text{n},\alpha)^7\text{Li}$  reaction produces two high-LET particles:  $^4\text{He}$  and  $^7\text{Li}$  (3, 4).

Nitrogen dose:  $^{14}\text{N}(\text{n},\text{p})^{14}\text{C}$  reaction produces high-LET proton.

Fast neutron dose: elastic scattering of neutrons by atomic nuclei of matter, mainly hydrogen, produces high-LET recoil nuclei, mainly protons. The last two doses are due to that abundant endogenous nuclei in the healthy tissue, such as  $^1\text{H}$  and  $^{14}\text{N}$ , that can capture neutrons yielding a gamma ray in the first case,  $^1\text{H}(\text{n},\gamma)^2\text{H}$ , and a proton in the second one,  $^{14}\text{N}(\text{n},\text{p})^{14}\text{C}$ . The reaction  $^{35}\text{Cl}(\text{n},\text{p})^{35}\text{S}$  gives a small contribution with high-LET proton also. However, the amount of radiation produced is less than that produced by the particle and recoiling nucleus in the case of boron (5).

Gamma quanta, which are a type of very high-frequency electromagnetic radiation, produce ionizations in the environment and living organism (1). Their penetrating power, in contrast to charged particles, is very high. The interaction of neutrons with matter takes place in a fundamentally different way. They interact not with the electron shells of the atom, but with the nucleus, transferring part of the energy to it. The escaped positively charged nucleus ionizes the media. In addition, a part of low-energy neutrons can be captured by the nucleus with the instantaneous emission of a gamma quantum or with the formation of new radioactive elements in the irradiated media.

In this way during the BNCT the damage of tissue is due to three types of directly ionizing radiations that differ in their LET characteristics (4). Low-LET gamma rays, resulting primarily from the capture of thermal neutrons by hydrogen atoms in tissue, [ $^1\text{H}(\text{n},\gamma)^2\text{H}$ ], but also present as incident gammas in the beam. High-LET protons and high-LET heavier charged particles ( $^4\text{He}$ ,  $^7\text{Li}$ ,  $^{14}\text{C}$ ), released as products of capture reactions in  $^{10}\text{B}$  and  $^{14}\text{N}$ : [ $^{10}\text{B}(\text{n},\alpha)^7\text{Li}$ ] and [ $^{14}\text{N}(\text{n},\text{p})^{14}\text{C}$ ], are mentioned above. In the case of low-

<sup>1</sup> Address for correspondence: Institute of Chemical Biology and Fundamental Medicine Siberian Branch of the Russian Academy of Sciences, Lavrentjeva Av. 8, Novosibirsk, 630090, Russia; email: maya.a.rot@gmail.com.

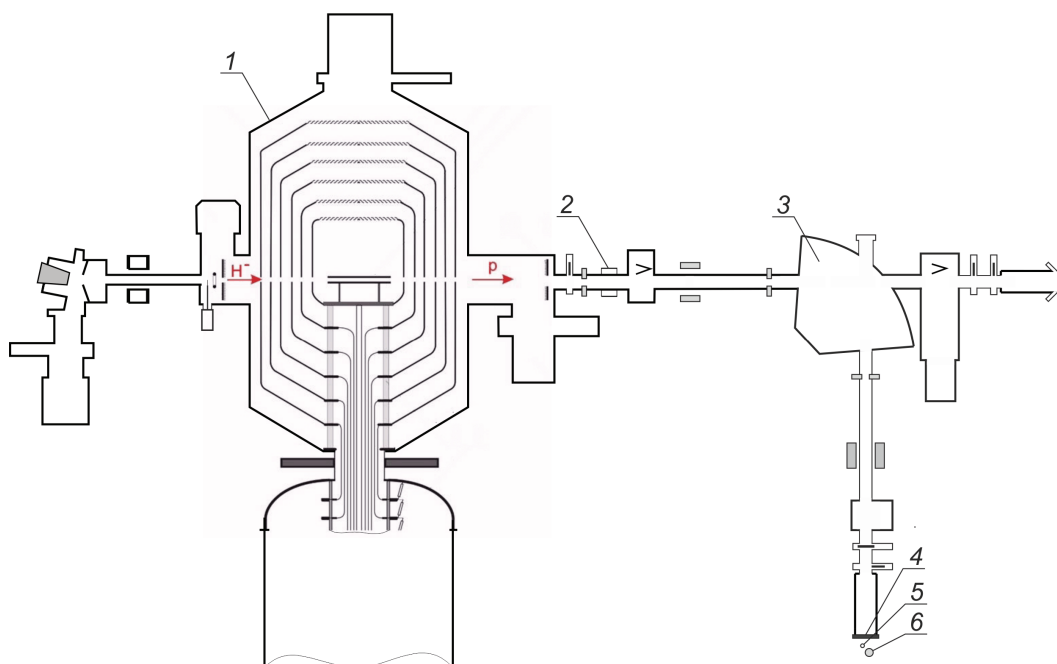


**FIG. 1.** Neutron source. 1. Vacuum insulated tandem accelerator. 2. Non-destructive DC current transformer. 3. Bending magnet. 4. Lithium target. 5. Cells. 6. Gamma-ray dosimeter.

LET radiation, lowering the dose rate is thought to reduce late effects in normal tissue much more than it decreases tumor control (6). The dose, which is due to high-LET particles produced in the reactions of absorption and scattering of neutrons, can be combined.

The idea for the approach to measure dose from high-LET particles is as follows (7). The cell lines are exposed to gamma rays and mixed radiation (neutrons and gamma rays), measuring  $\gamma$ -ray dose. The  $\gamma$ -ray doses, which cause the same effect, e.g., cell survival, are compared. The equivalent dose of high-LET particles is calculated using the formula:  $D_n = D_{\gamma \text{ standard}} - D_{\gamma \text{ mixed}}$ , where  $D_n$  is the equivalent dose of high-LET particles,  $D_{\gamma \text{ standard}}$  is the  $\gamma$ -ray dose when the cells are exposed to gamma rays, and  $D_{\gamma \text{ mixed}}$  is the dose of gamma radiation when the cells are exposed to mixed radiation. For clarity, we define equivalent dose as the absorbed dose multiplied by the radiation weighting factor, which is dependent on the type and energy of the radiation.

It is well known (8–10) that cell survival depends on the absorbed dose, time of irradiation, cell line culture, type of ionizing radiation and its energy spectrum. The proposed dose measurement method is free from the need to take into account all these dependencies. In the proposed method, it is required to achieve the same survival rate of the cell line, cell culturing conditions, the type of ionizing, gamma rays and mixed radiation, for the same time. If irradiation of cell cultures of the same line with two different types of radiation for the same time leads to the same cell survival, then the equivalent doses are equal.

## MATERIALS AND METHODS

### Cell Lines

The human glioblastoma multiforme cell line U251 was obtained from the Russian cell culture collection (Russian Branch of the ETCS, St. Petersburg, Russia). Cells were cultured in Minimum Essential Media (MEM) (Gibco® Grand Island, NY) supplemented with 10% (v/v) of fetal bovine serum (Gibco) and 1% (v/v) antibiotic-antimycotic solution (Gibco). Cells were maintained at 37°C in a 5% CO<sub>2</sub> atmosphere.

### Clonogenic Assay

Cells were seeded in six-well plates (TPP, Trasadingen, Switzerland) at a density of 300 cells per well after irradiation, incubated at 37°C in a humidified incubator under 5% (v/v) CO<sub>2</sub> for a week. Colonies were fixed with glutaraldehyde (6.0% v/v) and stained with crystal violet (0.5% w/v) (11). Colonies of more than 50 cells were counted. The percentage plating efficiency and surviving fraction were calculated based on a formula described elsewhere (11).

### Statistical Analyses

Outcome variables are expressed as means  $\pm$  standard deviations (SDs). Each experiment was repeated at least three times. Statistical analysis was performed using GraphPad Prism version 6.01 (GraphPad Software, San Diego, CA). Linear regression and paired *t* test were used for data analysis. Probability values of *P* < 0.05 were considered statistically significant.

### Irradiation Facility

The cells were irradiated at an accelerator-based neutron source of the Budker Institute of Nuclear Physics in Novosibirsk, Russia (12). A schematic of the source is shown in Fig. 1. The neutron source comprises an original design tandem accelerator (no. 1 in Fig. 1) to provide up to 2.3 MeV, 10 mA proton beam, an advanced solid lithium target (no. 4) to generate neutrons by  ${}^7\text{Li}(p,n){}^7\text{Be}$  threshold



**FIG. 2.** Experimental setup equipment. 1. Lithium target assembly. 2. Copper substrate. 3. Aluminum disc. 4. Cells in flasks. 5. Gamma-ray dosimeter. The inscription in Russian («осторожно радиация!») translates as “caution radiation”.

reaction, and beam shaping assembly (not shown) to form therapeutic flux of epithermal neutrons (13). The lithium target (no. 4 in Fig. 1) has three layers: a thin layer of pure lithium to generate neutrons in  ${}^7\text{Li}(p,n){}^7\text{Be}$  reaction; a thin layer of material resistant to radiation blistering; and a thin copper substrate for efficient heat removal (14). A lithium layer thickness of 200  $\mu\text{m}$  was evaporated onto the target on a separate stand. When evaporating natural lithium is used, in which the lithium-6 isotope is contained in a concentration of 7.5%, lithium-7 is at 92.5%. The percentage of lithium isotopes is taken into account below in the reported values of the neutron yield and 478 keV photon yield from the lithium target (15). In this experiment, as shown in Fig. 1, the cryotubes (TPP) with cells, (no. 5), are placed below the lithium target. A total of  $0.5 \times 10^6$  cells in 1 ml of complete culture media were contained in each cryotube. Irradiated and control cells underwent the same conditions, inside the bunker at RT, with the only difference that the control cells were placed further from the radiation generation site and fenced off with concrete blocks. The ambient  $\gamma$ -ray dose rate was measured using a DBG-S11D dosimeter (Doza, Russia) (no. 6 in Fig. 1) with 15% accuracy. The proton beam current was measured and controlled by a non-destructive DC current transformer (NPCT, Bergoz Instrumentation, Saint-Genis-Pouilly, France) (no. 2 in Fig. 1) The position and size of proton beam at the surface of the lithium target were controlled using a Hikvision video camera (Hangzhou, China) through the window in the target unit. Neutrons were detected using a BDMN dosimeter (Doza, Russia) and a detector with a GS20 lithium-containing scintillator (Saint-Gobain Crystals, Malvern, PA).

The cells were irradiated in two modes: with energy of protons equal to 1.8 MeV and 2.05 MeV. In the first case, the cells were exposed to gamma-quanta with energy of 478 keV generated as a result of inelastic scattering of protons by lithium atomic nuclei (the  ${}^7\text{Li}(p,p'\gamma){}^7\text{Li}$  reaction). In the second case, the neutrons were added by the  ${}^7\text{Li}(p,n){}^7\text{Be}$  threshold reaction (threshold energy is 1.882 MeV). The protons are stopped in the lithium layer.

## RESULTS AND DISCUSSION

### Gamma-Ray Irradiation

To estimate the doses, we used the glioblastoma cell line U251, which was previously used in experiments with BNCT, particularly in clonogenic studies (16). The last one is the survival assay, which is based on the ability of a single cell to grow into a colony (11). First, U251 cells were

irradiated only with gamma rays, and their survival was determined. The experimental setup is shown in Fig. 2.

A flux of 478 keV photons was produced in the  ${}^7\text{Li}(p,p'\gamma){}^7\text{Li}$  reaction at a proton beam energy below 1.882 MeV, the threshold of the  ${}^7\text{Li}(p,n){}^7\text{Be}$  reaction. A 200- $\mu\text{m}$  thick lithium layer was deposited on a copper substrate with cooling channels (no. 2 in Fig. 2) which was pressed against a planar aluminum disc (no. 3 in Fig. 2). A proton beam 3 cm in diameter was directed to the target and 478 keV photons were produced. Cell cultures in flasks and the dosimeter (nos. 4 and 5 in Fig. 2, respectively) were placed under the target.

The U251 cell line was irradiated for 1.5 h with photons produced in the  ${}^7\text{Li}(p,p'\gamma){}^7\text{Li}$  reaction at a proton energy of  $1.800 \pm 0.002$  MeV and proton current of  $2.17 \pm 0.03$  mA.

The dose absorbed by the cells was 5.21 Gy. This was measured as follows. The dose measured with the gamma-ray dosimeter was 1.16 Gy. Since the gamma-ray dosimeter and the cells were located similarly from the irradiated area, but at different distances, it can be assumed that their doses differ as the square of the distances. Assuming that the distance from the center of the photon emission region to the cells is 5 cm, and to the dosimeter it is 10.6 cm, then  $1.16 \times (10.6/5)^2 = 5.21$  Gy.

A value close to this, 5.25 Gy, was obtained as a result of numerical simulation of  $\gamma$ -ray transport by the method described elsewhere (13). The yield of photons from natural lithium was assumed to be  $0.756 \cdot 10^{14} \text{ C}^{-1}$ , measured at the facility in BINP. The results from measuring the photon yield from a thick lithium target will be reported in a future article.

After  $\gamma$ -ray irradiation the surviving fractions of the U251 cell line were examined using a clonogenic assay. The surviving fraction (SF) was calculated as described elsewhere (11). Cell surviving curves were obtained after neutron irradiation according to the linear-quadratic model. Cell survival as a result of photon irradiation was  $34 \pm 4\%$ .

### Mixed Irradiation

To generate mixed radiation (neutrons and gamma rays), the proton energy was increased to 2.05 MeV, above the threshold of the  ${}^7\text{Li}(p,n){}^7\text{Be}$  reaction.

At an energy of 2.05 MeV, the neutron yield from a lithium target as a result of the  ${}^7\text{Li}(p,n){}^7\text{Be}$  reaction is  $1.53 \cdot 10^{11} \text{ mC}^{-1}$ , the average neutron energy is 90 keV and the maximum is 290 keV (15). The yield of 478-keV photons from a lithium target at a proton energy of 2.05 MeV is  $1.18 \cdot 10^{11} \text{ mC}^{-1}$ . Although the yield of neutrons exceeds the yield of photons by 1.3 times, due to the significantly higher kerma factor of neutrons compared with a kerma factor of 478 keV photons (17), the fast neutron dose is 19 times higher than the  $\gamma$ -ray dose, as obtained in the simulations.

A plexiglass moderator is applied to convert this neutron flux into a beam of thermal neutrons suitable for *in vitro* and

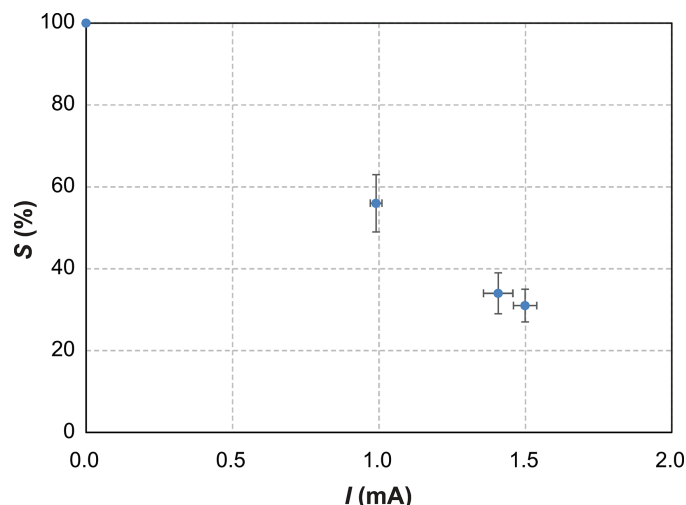


FIG. 3. The dependence of survival,  $S$ , on the proton beam current,  $I$ .

*in vivo* studies of the BNCT technique (15, 18). This allows for a significant reduction in the fast neutron dose.

In this experiment, a plexiglass cylinder with 200-mm diameter and 72-mm thickness was installed close to the target. Its placement required moving the cells away from the radiation generation area up to 10.6 cm and the dosimeter up to 15.9 cm. The placement of the plexiglass moderator also led to the appearance of additional 2.2-MeV gamma rays caused by neutron capture by hydrogen [ $H(n,\gamma)^2H$ ].

The experiment scenario was as follows. A certain value of the proton beam current was set, the cells were irradiated for 1.5 h and then their survival was determined. If the cell survival was more than 34%, then in the next irradiation the beam current would be increased; if it was less, then it would be reduced. The dependence of survival  $S$  on the proton beam current  $I$  is shown in Fig. 3. At a current of  $0.99 \pm 0.02$  mA, the survival fraction was  $54 \pm 7\%$ , at  $1.50 \pm 0.04$  mA –  $31 \pm 4\%$ , and finally at  $1.40 \pm 0.05$  mA the cell survival fraction was achieved at exactly 34%. In this case, the proton energy was  $2.050 \pm 0.002$  MeV.

Using the gamma-ray dosimeter, the measured dose was 1.77 Gy under irradiation with a proton current of 1.40 mA. Assuming similarly that the dose in the cells and the dose measured by the dosimeter differ as the square of the distances, we obtained the  $\gamma$ -ray dose absorbed by the cells equal to  $1.77 \times (15.9/10.6)^2 = 3.98$  Gy.

Since the survival rate of cells after exposure to mixed radiation is the same as that of gamma rays and the irradiation times were equal, the cells received the same equivalent dose of 5.21 Gy-Eq. When exposed to mixed radiation, gamma rays gave 3.98 Gy-Eq at this dose, indicating that the remaining 1.23 Gy-Eq were due to recoil nuclei caused by the absorption of thermal neutrons and elastic scattering of fast neutrons.

The result obtained has a practical value: It facilitates the assessment of the effect caused by radiation, namely, when carrying out such irradiation, it is sufficient to measure only the  $\gamma$ -ray dose and assume that the sum of fast neutron doses and nitrogen doses is equal to 31% of the  $\gamma$ -ray dose.

Of course, the proposed method can be used to measure the boron dose, but it turned out that it is easier and more reliable to measure it using our developed small-sized neutron detector with a polystyrene cast scintillator with boron (19). The results of measuring the spatial distribution of the boron dose have been reported elsewhere (20, 21)

Thus, all four components of the equivalent dose can be measured: the  $\gamma$ -ray dose, with gamma-ray dosimeters; the boron dose, using a neutron detector with a polystyrene cast scintillator with boron; and the sum of the fast neutron dose and nitrogen dose, using the method described above.

## CONCLUSIONS

In boron neutron capture therapy, the total absorbed dose is the sum of four dose components with different RBE: high-LET boron dose; high-LET dose from the  $^{14}N(n,p)^{14}C$  reaction (“nitrogen” dose); high-LET fast neutron dose; and  $\gamma$ -ray dose. For measuring nitrogen dose and fast neutron dose we proposed a new approach. Here, the cell lines receive  $\gamma$ -ray and mixed irradiation (i.e., neutrons and  $\gamma$  rays) for the same time, measuring  $\gamma$ -ray dose. After that, by comparing the  $\gamma$ -ray doses causing the same effect, e.g., survival, we determine the doses due to high-LET particles. The results presented in this work demonstrate the applicability of the proposed approach for measuring the equivalent dose components due to neutrons: nitrogen dose, and fast neutron dose.

## ACKNOWLEDGMENTS

This research was funded by the Russian Science Foundation, grant no. 19-72-30005. A patent for the proposed method was received; priority date was June 1, 2020.

Received: January 21, 2021; accepted: May 6, 2021; published online: May 21, 2021

## REFERENCES

1. Powsner RA, Powsner ER. Essential nuclear medicine physics. Hoboken, NJ: John Wiley & Sons; 2008.
2. Rassow J, Sauerwein WAG. Prescribing, recording and reporting of BNCT. In: Sauerwein WAG, Wittig A, Moss R, Nakagawa Y. Neutron capture therapy: Principles and applications: Springer; 2012. p. 277–87.
3. Sauerwein WAG. Principles and roots of neutron capture therapy. In: Sauerwein WAG, Wittig A, Moss R, Nakagawa Y. Neutron Capture Therapy: Principles and Applications. Berlin: Springer; 2012. p. 1–18.
4. Coderre JA, Turcotte JC, Riley KJ, Binns PJ, Harling OK, Kiger WS 3rd. Boron neutron capture therapy: Cellular targeting of high linear energy transfer radiation. Technol Cancer Res Treat 2003; 2:355–75.

5. Cerecetto H, Couto M. Medicinal chemistry of boron-bearing compounds for BNCT-glioma treatment: Current challenges and perspectives. In: Omerhodzic I, Arnautovic K, editors. Glioma – Contemporary diagnostic and therapeutic approaches. IntechOpen 2018.
6. Masunaga SI, Kobayashi J, Tano K, Sanada Y, Suzuki M, Ono K. The effect of p53 status on radio-sensitivity of quiescent tumor cell population irradiated with g-rays at various dose rates. *J Clin Med Res* 2018; 10:815–21.
7. Taskaeva I, Taskaev S. Method of measuring of dose produced by recoil nuclei. Patent for invention No. 2743417; 18 February 2021.
8. Yura Y, Fujita Y. Boron neutron capture therapy as a novel modality of radiotherapy for oral cancer: Principle and antitumor effect. *Oral Sci Int* 2013; 10:9–14.
9. Wang P, Zhen H, Jiang X, Zhang W, Cheng X, Guo G, et al. Boron neutron capture therapy induces apoptosis of glioma cells through Bcl-2/Bax. *BMC Cancer* 2010; 10:661.
10. Faiao-Flores F, Coelho PR, Arruda-Neto JD, Maria-Engler SS, Maria DA. Cell cycle arrest, extracellular matrix changes and intrinsic apoptosis in human melanoma cells are induced by boron neutron capture therapy. *Toxicol Vitr* 2013;27, DOI: 10.1016/j.tiv.2013.02.006.
11. Franken NA, Rodermond HM, Stap J, Haveman J, van Bree C. Clonogenic assay of cells in vitro. *Nat Protoc* 2006; 1:2315–9.
12. Taskaev SY. Accelerator based epithermal neutron source. *Phys Part Nucl* 2015; 46:956–90.
13. Zaidi L, Belgaid M, Taskaev S, Khelili R. Beam shaping assembly design of  $7\text{Li}(p,n)7\text{Be}$  neutron source for boron neutron capture therapy of deep-seated tumor. *Appl Radiat Isot* 2018; 139:316–24.
14. Bayanov B, Belov V, Kindyuk V, Oparin E, Taskaev S. Lithium neutron producing target for BINP accelerator-based neutron source. *Appl Radiat Isot* 2004; 61:817–21.
15. Lee CL, Zhou XL. Thick target neutron yields for the  $7\text{Li}(p,n)7\text{Be}$  reaction near threshold. *Nucl Instrum Methods Phys Res B* 1999; 152:1–11.
16. Sato E, Zaboronok A, Yamamoto T, Nakai K, Taskaev S, Volkova O, et al. Radiobiological response of U251MG, CHO-K1 and V79 cell lines to accelerator-based boron neutron capture therapy. *J Radiat Res* 2018; 59:101–7.
17. Kiger III WS, Kumada H. Treatment planning. In: Sauerwein WAG, Wittig A, Moss R, Nakagawa Y, editors. Neutron capture therapy: Principles and applications. Berlin: Springer; 2012. p.287–326.
18. Zavjalov E, Zaboronok A, Kanygin V, Kasatova A, Kichigin A, Mukhamadiyarov R, et al. Accelerator-based boron neutron capture therapy for malignant glioma: a pilot neutron irradiation study using boron phenylalanine, sodium borocaptate and liposomal borocaptate with a heterotopic U87 glioblastoma model in SCID mice. *Int J Radiat Biol* 2020; 96:868–78.
19. Bykov TA, Kasatov DA, Koshkarev AM, Makarov AN, Porosev VV, Savinov GA, et al. A multichannel neutron flux monitoring system for a boron neutron capture therapy facility. *JINST* 2019; 14:P12002.
20. Bykov TA, Kasatov DA, Koshkarev AM, Makarov AN, Porosev VV, Savinov GA, et al. Initial trials of a dose monitoring detector for boron neutron capture therapy. *JINST* 2021; 16:P01024.
21. Taskaev S, Berendelev E, Bikchurina M, Bykov T, Kasatov D, et al. Neutron source based on vacuum insulated tandem accelerator and lithium target. *Biology (Basel)* 2021; 10:350.